Boundary tension of 2D and 3D Ising models

Harold J.W. Zandvliet[1] and Cornelis Hoede[2]

[1]Physical aspects of Nanoelectronics & MESA+ Institute for Nanotechnology, University of Twente, P.O. Box 217, 7500 AE Enschede, The Netherlands

[2]Department of Applied Mathematics, University of Twente, P.O. Box 217, 7500 AE Enschede, The Netherlands

A simple route to determine the boundary tension of Ising models is proposed. As pointed out by Onsager, the boundary tension is an important quantity since it vanishes at the critical temperature and can thus be used to determine the critical temperature. Here we derive expressions for the boundary tension along various high symmetry directions of the anisotropic square and triangular lattices. The exact results by respectively Onsager (Phys. Rev. **65**, 117 (1944)) for the anisotropic square lattice and by Houtappel (Physica **16**, 435 (1950)) for the anisotropic triangular lattice are reproduced. Subsequently, we will apply our method to Ising models that have not been exactly solved yet. Valuable results are obtained for the 2D square Ising lattice with nearest and weak next-nearest neighbour interactions as well as for the strongly anisotropic 3D Ising lattice.

PACS numbers: 64.60.-i, 64.60.De

The square Ising lattice with nearest-neighbour interactions has been exactly solved by Onsager in 1944 [1]. A few years later Houtappel solved the anisotropic triangular lattice [2]. These two-dimensional Ising models have served as a cornerstone for critical-point theory and as a playground for many approximate theoretical models. However, if an applied magnetic field or next-nearest neighbour interaction is included these models can no longer be solved exactly with presently available theoretical techniques.

Since Onsager's contribution there has been a substantial activity in the field of two-dimensional Ising models having interactions that go beyond nearest neighbours or involve different symmetries, since it is predicted that all these planar models fall in the same universality class. Despite the fact that these models are defined simply, most of them exhibit rather rich phase diagrams.

The square Ising model with nearest- and next-nearest neighbour interactions has been investigated by various techniques: series expansion [3], Monte Carlo [4,5], renormalization group [6], Monte Carlo renormalization [7] and finite-size scaling [8,9]. The available theoretical data have resulted in a global phase diagram of this Ising model [10,11]. In ref. [10] closed-form empirical expressions are given that represent the phase boundaries between the various phases (ferromagnetic, antiferromagnetic, superantiferromagnetic and paramagnetic) rather well.

Here we put forward a simple method to determine the phase boundaries between the different phases in the phase diagram. The method relies on the derivation of an expression for the domain wall free energy also referred as boundary tension that separates regions with the "right" spin ordering from regions with the "wrong" spin ordering [12-17]. In case of the anisotropic square

and triangular lattices with nearest neighbour interactions this method leads to the well-known exact results obtained by Onsager [1] and Houtappel [2]. The obtained phase diagram of the square lattice with nearest and next-nearest neighbour interactions is not exact, but it is astonishingly accurate in the parameter region where the nearest neighbour coupling is stronger than the next-nearest neighbour coupling. For a vanishing next-nearest neighbour interaction the obtained result is even asymptotically exact.

The boundary tension method is also applicable to the cubic 3D Ising lattice. Although this approach only leads to a lower bound for the critical temperature of the isotropic 3D Ising model, it gives an asymptotically exact result for the anisotropic lattice, where the coupling constant in one direction is much stronger than the coupling constants in the other two directions.

1. The boundary tension method and some exact results.

We start with the derivation of the boundary tension (or boundary free energy) along the high symmetry [10] direction, $F_{(10)}$, of a square 2D Ising model with crossing bonds. For the sake of simplicity we will restrict ourselves here to a simple square 2D lattice with isotropic ferromagnetic nearest neighbour interactions ($J>0$). The next-nearest-neighbour interaction (J_d) can either be ferromagnetic or antiferromagnetic. We consider a boundary running along the [10] direction that separates two regions with opposite spins. At zero temperature the boundary is kinkless and the formation energy per unit spin or unit length is given by, $E_{(10)} = 2J + 4J_d$. With increasing temperature the formation of kinks in the boundary allows the boundary to wander (see Fig. 1).

This wandering increases the entropy and thus lowers the free energy of the boundary. However, the creation of kinks in the boundary costs energy and thus increases the energy of the boundary. The formation energy of a kink with length n (measured in spins) in a [10] boundary is given by, $E_{n,(10)} = 2nJ + 4(n-1)J_d$ [18]. In Fig.1 the various pathways that we have taken into account are depicted. The partition function of the [10] boundary per spin is then,

$$Z_{(10)} = \sum_i e^{-E_i/k_BT} = e^{-2(J+2J_d)/k_BT}\left[1+2\sum_{n=1}^{\infty} e^{-(2nJ+4(n-1)J_d)/k_BT}\right], \qquad (1)$$

where we have summed over all possible configurations of an elementary boundary segment. The boundary free energy per spin or boundary tension can be derived from the expression, $F_{(10)} = -k_BT \ln\left[Z_{(10)}\right]$. We find

$$F_{(10)} = 2J + 4J_d - k_BT \ln\left[1+\frac{2e^{-2J/k_BT}}{1-e^{-(2J+4J_d)/k_BT}}\right]. \qquad (2)$$

For the square 2D Ising lattice with anisotropic nearest neighbour and isotropic next-nearest neighbour couplings we find,

$$F_{(10)} = 2J_y + 4J_d - k_BT \ln\left[1+\frac{2e^{-2J_x/k_BT}}{1-e^{-(2J_x+4J_d)/k_BT}}\right] \qquad (3a)$$

and

$$F_{(01)} = 2J_x + 4J_d - k_B T \ln\left[1 + \frac{2e^{-2J_y/k_B T}}{1 - e^{-\left(2J_y + 4J_d\right)/k_B T}}\right] \qquad \text{(3b)},$$

for the [10] and [01] directions, respectively. The critical temperature can be found by setting Eq. 3(a) or 3(b) equal to zero.

$$e^{-2J_x/k_B T_c} + e^{-2J_y/k_B T_c} + e^{-2\left(J_x + J_y\right)/k_B T_c}\left(2 - e^{-4J_d/k_B T_c}\right) = e^{4J_d/k_B T_c}. \qquad (4)$$

For a vanishing next-nearest-neighbor interaction the original result of Onsager, i.e. $F_{(10,01)} = 2J_{y,x} - k_B T \ln\left[\frac{1 + e^{-2J_{x,y}/k_B T}}{1 - e^{-2J_{x,y}/k_B T}}\right]$, is recovered. This is intriguing since we have ignored overhangs and inclusions in the partition function (see Fig. 1). Despite this severe limitation the boundary tension is correct for *any* temperature, suggesting that our partition function contains the correct set of Boltzmann factors. The only way to understand this is that the contributions of overhangs and inclusions nicely cancel each other at *any* temperature. By setting the boundary tension equal to zero we find Onsager's criticality condition, i.e.,

$$\sinh\left(\frac{2J_x}{k_B T_c}\right)\sinh\left(\frac{2J_y}{k_B T_c}\right) = 1 \qquad (5)$$

In a similar manner the free energy of a boundary running along the [11] direction can be derived. If overhangs and inclusions are ignored we find (see Fig. 2).

$$Z_{(11)} = \sum_i e^{-E_i/k_BT} = \left(e^{-2J_x/k_BT} + e^{-2J_y/k_BT} \right) \left[\sum_{n=1}^{\infty} e^{-2n\left(J_x+J_y\right)/k_BT} \right] \tag{6}$$

The partition sum $Z_{(11)}$ can be rewritten in form

$$Z_{(11)} = \frac{e^{-2J_x/k_BT} + e^{-2J_y/k_BT}}{1 - e^{-2(J_x+J_y)/k_BT}} \tag{7}$$

The boundary tension per spin or per unit length, a (a is the nearest-neighbor distance between the spins) along the [11] direction is then,

$$F_{(11)} = -\sqrt{2}k_BT \ln\left(Z_{(11)}\right) \tag{8}$$

The critical temperature is found by setting $F_{(11)} = 0$ or $Z_{(11)} = 1$. We find,

$$e^{-2J_x/k_BT_c} + e^{-2J_y/k_BT_c} + e^{-2\left(J_x+J_y\right)/k_BT_c} = 1 \tag{9}$$

or again,

$$\sinh\left(\frac{2J_x}{k_BT_c}\right)\sinh\left(\frac{2J_y}{k_BT_c}\right) = 1 \tag{10}$$

Recently, Schumann and Kobe [16] applied the above mentioned method to determine the partition function of a [10] boundary of the fully anisotropic 2D square Ising model with both nearest $\left(J_x, J_y\right)$ and next-nearest neighbour interactions $\left(J_{d1}, J_{d2}\right)$. They found by using our approach,

$$Z_{(10)} = e^{-2(J_y+J_{d1}+J_{d2})/k_BT}\left(1+\left(e^{4J_x/k_BT}+e^{4J_y/k_BT}\right)\frac{e^{-2(J_x+J_{d1}+J_{d2})/k_BT}}{1-e^{-2(J_x+J_{d1}+J_{d2})/k_BT}}\right) \tag{11}$$

For $J_{d1}=0$ (or $J_{d2}=0$) the fully anisotropic 2D square model reduces to the anisotropic triangular lattice with coupling constants J_x, J_y and J_z. The equation giving the critical temperature is identical to the criticality condition derived by Houtappel [2], i.e.,

$$e^{-2(J_x+J_y)/k_BT_c}+e^{-2(J_x+J_z)/k_BT_c}+e^{-2(J_y+J_z)/k_BT_c}=1 \tag{12}$$

The latter expression is equivalent to,

$$\sinh\left(\frac{2J_x}{k_BT_c}\right)\sinh\left(\frac{2J_y}{k_BT_c}\right)+\sinh\left(\frac{2J_x}{k_BT_c}\right)\sinh\left(\frac{2J_z}{k_BT_c}\right)+\sinh\left(\frac{2J_y}{k_BT_c}\right)\sinh\left(\frac{2J_z}{k_BT_c}\right)=1 \tag{13}$$

In Table I an overview of the exact solutions of square and triangular Ising lattices as well as the criticality condition obtained from the expressions for the boundary tension along the [10] and [11] directions are given.

	Exact	[10] boundary	[11] boundary
Isotropic 2D square	$S=1$ [1]	$S=1$ [15]	$S=1$
Anisotropic 2D square	$S_xS_y=1$ [1]	$S_xS_y=1$ [15]	$S_xS_y=1$
Isotropic triangular	$3S^2=1$ [2]	$3S^2=1$ [15]	$3S^2=1$
Anisotropic triangular	$S_xS_y+S_xS_z+S_yS_z=$ [2]	$S_xS_y+S_xS_z+S_yS_z=1$ [16]	$S_xS_y+S_xS_z+S_yS_z=1$

Table I

Comparison of criticality conditions of the exact solutions of various planar Ising models and results obtained by the "boundary tension" method. $\left(S=\sinh\left(\frac{2J}{k_BT_c}\right)\right)$.

2. The phase diagram of the 2D square Ising lattice with nearest and next-nearest neighbour interactions

So far we have only determined the phase boundary that separates the ferromagnetic from the paramagnetic phase. The other two phase boundaries, i.e. the phase boundaries between the antiferromagnetic and paramagnetic and between the superantiferromagnetic and paramagnetic phases can be extracted as well. For the sake of simplicity we restrict ourselves to the 2D square lattice with isotropic nearest (J_{NN}) and isotropic next-nearest neighbour (J_{NNN}) interactions. The phase boundary between the antiferromagnetic phase and paramagnetic phase can simply be found by replacing J_{NN} by $|J_{NN}|$. One finds,

$$2e^{-2|J_{NN}|/k_BT_c} + e^{-4|J_{NN}|/k_BT_c}\left(2 - e^{-4J_{NNN}/k_BT_c}\right) = e^{4J_{NNN}/k_BT_c} \quad . \qquad (14)$$

Next we consider the superantiferromagnetic phase. We consider a domain wall running along the *x*-direction (the [10] direction) of the superantiferromagnetic phase. As we will see later on, it does not matter whether the striped spin domains of the superantiferromagnetic phase run along or are perpendicular to the direction of the domain wall (here we assume that in the *x*-direction the nearest neighbour coupling is ferromagnetic and in the *y*-direction the nearest neighbour coupling is antiferromagnetic).

The domain wall formation energy per unit length along the *x*-direction is,

$$E_{(10)} = -2J_y - 4J_d = 2J_{NN} - 4J_{NNN} \quad . \qquad (15)$$

The superantiferromagnetic state will be the ground state if the domain wall energy is positive, i.e. $J_{NNN} \le -\frac{1}{2} J_{NN}$ ($J_y = -J_{NN} < 0$ and $J_d = J_{NNN} < 0$). At zero temperature, the domain wall is always as straight as possible. However, with increasing temperature the formation of thermally excited kinks allows the domain wall to wander, increasing the entropy and thus decreasing the free energy for domain wall formation [15]. The formation energy of a kink with length n (measured in units a) in a [10] boundary is given by

$$E_{n,(10)} = 2nJ_x - 4(n-1)J_d = 2nJ_{NN} - 4(n-1)J_{NNN} \qquad \text{with } n \ge 1. \tag{16}$$

The partition function of the superantiferromagnetic domain wall is

$$Z_{(10)} = \sum_i e^{-E_i / k_B T} = e^{-(2J_{NN} - 4J_{NNN}))/k_B T} \left(1 + 2 \sum_{n=1}^{\infty} e^{-(2nJ_{NN} - 4(n-1)J_{NNN})/k_B T} \right). \tag{17}$$

Here we have summed over all possible configurations of an elementary boundary segment. In this approach overhangs and inclusions are again explicitly excluded.

The superantiferromagnetic to paramagnetic phase boundary can be determined by setting the domain wall free energy, $F_{(10)} = -k_B T \ln(Z_{(10)})$, equal to zero. This results in the following equation,

$$e^{-2J_{NN}/k_B T_c} + e^{2J_{NN}/k_B T_c} + \left(2 - e^{4J_{NNN}/k_B T_c}\right) = e^{-4J_{NNN}/kBT_c}.$$

(18)

The superantiferromagnetic to paramagnetic phase boundary can then be rewritten as

$$\cosh\left(\frac{2J_{NN}}{k_bT_c}\right)+1=\cosh\left(\frac{4J_{NNN}}{k_bT_c}\right) \quad \text{and} \quad J_{NNN}<0. \tag{19}$$

Exactly the same result is found if we consider a domain wall running in the [01] direction, i.e. perpendicular to the striped spin up or spin down regions. Eq. (19) is exactly the same as the expression derived earlier by Fan and Wu [19] within the framework of the free-fermion model. Eqs. (14) and (19) give the full phase diagram of the square 2D Ising model with isotropic nearest- and next-nearest-neighbor interactions.

In Fig. 3 a plot of the phase diagram is shown. All the phase boundaries of this Ising model exhibit asymptotic behavior in the strong coupling limit ($J_{NNN}\to-\frac{1}{2}|J_{NN}|$). The latter is in agreement with predictions from a renormalization analysis [5]. The data points are series expansions results (triangles, Oitmaa [3]), finite scaling of transfer matrix results (squares, Nightingale [20,21]), Onsager's exact result (filled circles, Onsager [1]), Monte Carlo simulations (open circles, Blöte, Compagner and Hoogland [12] and open stars, Landau [4]) and free-fermion approximation (closed stars, Fan and Wu [19]). The agreement between the available numerical and theoretical data and our domain result wall is very good in the strong coupling limit. However, it

must be noted that in the weak nearest neighbour coupling limit our result deviates from the theoretical data. For a vanishing nearest neighbour interaction (i.e. $J_{NN} \to 0$), our approach gives $J_{NNN}/k_bT_c = -\frac{1}{2}\ln\left(\frac{\sqrt{2}}{\sqrt{3}-1}\right)$ (≈-0.3293) while the exact number should be $-\frac{1}{2}\ln\left(\sqrt{2}+1\right)$ (≈-0.4407). Despite this discrepancy, the result for the phase boundary correctly displays a maximum at J_{NN}/k_BT=0, which is consistent with the proposed phase diagram of this system.

In the Onsager point $\left(J_{NNN}=0\right)$ we find that the derivative $\left(\frac{\partial J_{NNN}}{\partial J_{NN}}\right)_{J_{NNN}=0}$ as determined from either the [10] or the [11] boundary tension is $-\frac{1}{2}\sqrt{2}$, which should be a property of the exact solution [13].

3. The ferromagnetic anisotropic 3D Ising lattice

In contrast to the 1D and the 2D Ising models, the 3D Ising model has, despite hugh efforts, not been solved exactly. It is evident that an exact solution of the 3D Ising model would be a great step forward, since it can be used to describe a broad class of phase transitions, ranging from binary alloys, simple liquids and their mixtures, polymer solutions to easy-axis magnets [22,23]. The first rigorous proof that the Ising model in three dimensions exhibits a phase transition in the sense of having a nonzero spontaneous magnetization below some critical temperature T_C was provided by Griffiths [24]. Griffiths made use of a heuristic argument that has been put forward and applied earlier by Peierls to the 2D case

[25]. A lower bound on the critical temperature of the anisotropic 3D Ising model where one coupling constant (J_z) is much larger than the coupling constants in the other 2 directions (J_x, J_y) was derived by Weng, Griffiths and Fisher [26]. With increasing exchange energy anisotropy the lower bound on the critical temperature decreases logarithmically,

$$\frac{k_B T_C}{J_z} = 2\left[\ln\left(\frac{J_z}{J_x + J_y} \right) - \ln\left(\ln\left(\frac{J_z}{J_x + J_y} \right) \right) + O(1) \right]^{-1} \quad . \qquad (20)$$

Weng, Griffiths and Fisher [26] surmised that Eq. (20) is even asymptotically exact. The latter was indeed confirmed in a subsequent paper by Fisher [27], where he derived an upper bound on the critical temperature, which has the exact form of Eq. (20).

We consider the anisotropic simple-cubic Ising lattice. The nearest-neighbour exchange energies between the spins in the *x*-, *y*- and *z*- direction are represented by J_x, J_y and J_z, respectively. For convenience we use the following notation,

$$H_x = \frac{J_x}{k_B T} \quad , \quad H_y = \frac{J_y}{k_B T} \quad \text{and} \quad H_z = \frac{J_z}{k_B T} \quad . \qquad (21)$$

For the sake of simplicity we assume that all the nearest neighbor interactions are ferromagnetic, i.e. $J_{x,y,z} > 0$. In order to derive an expression for the order-disorder phase transition temperature we consider to domains with opposite spin ordering. We assume that at zero temperature the domain wall is located in

the *xy*-plane. It should be pointed out here that this choice does not have any influence on our main conclusion. Each cell *(i,j)* of the domain wall is represented by a column in the *z*-direction with height $h(i, j)$ and is surrounded by four neighbours with indices *(i-1,j), (i+1,j), (i,j-1)* and *(i,j+1)* respectively (see Fig. 4). As is evident, the height differences between these columns directly affect the formation energy of the domain wall. The total partition sum of the domain wall, Z_{tot}, can be written as,

$$Z_{tot} = \sum_{m} e^{-E_m / k_B T} = \prod_{(i,j)} Z_{(i,j)}, \qquad (22)$$

where the summation *m* runs over all possible configurations of the domain wall and $Z_{(i,j)}$ is the partition sum of the *(i,j)-th* cell. We start with the assumption that $H_z >> H_{x,y}$. If overhangs and inclusions (i.e. droplets and bubbles of the opposite spin ordering) are ignored the following partition function of *(i,j)-th* cell, $Z_{(i,j)}$, can be derived [28];

$$Z_{(i,j)} = \sum_{h(i,j)=-\infty}^{\infty} e^{-\left(2H_z + 2H_x \left|h(i,j)-h(i-1,j)\right| + 2H_y \left|h(i,j)-h(i,j-1)\right|\right)}. \qquad (23)$$

The summation in Eq. (4) can be separated into three terms

$$Z_{(i,j)} = e^{-2H_z} \sum_{h(i,j)=-\infty}^{-1} e^{2h(i,j)(H_x+H_y) - 2\left|\bar{h}\right| H_y} +$$

$$e^{-2H_z}\sum_{h(i,j)=0}^{|\bar{h}|} e^{-2h(i,j)H_X-2(|\bar{h}|-h(i,j))H_y} + e^{-2H_z}\sum_{h(i,j)=|\bar{h}|+1}^{\infty} e^{-2(h(i,j)-|\bar{h}|)(H_X+H_y)-2|\bar{h}|H_X}$$

(24)

where $\bar{h} = h(i-1, j) - h(i, j-1)$ (see Fig. 4).

It is convenient to replace $h(i, j)$ by n and rearrange Eq. (24) to

$$Z_{(i,j)} = e^{-2H_z}\left[\sum_{n=0}^{|\bar{h}|} e^{-2nH_X-2(|\bar{h}|-n)H_y} + \left(e^{-2|\bar{h}|H_X} + e^{-2|\bar{h}|H_y}\right)\sum_{n=1}^{\infty} e^{-2n(H_X+H_y)}\right]$$

(25)

All three terms deal with the energy that is required to form the side planes of the column $h(i, j)$. The probabilities of finding an upward or downward excitation are equal and therefore the mean overall orientation of the domain wall is maintained parallel to the *xy*-plane. Eq. (25) can be rewritten to,

$$Z_{(i,j)} = e^{-2H_z}\left[\left(\frac{e^{-2(|\bar{h}|+1)H_X} - e^{-2(|\bar{h}|+1)H_y}}{e^{-2H_X} - e^{-2H_y}}\right) + \left(\frac{(e^{-2|\bar{h}|H_X} + e^{-2|\bar{h}|H_y})e^{-2(H_X+H_y)}}{1-e^{-2(H_X+H_y)}}\right)\right]$$

(26)

It is convenient to introduce the following variables;

$$u = e^{-2H_x},\ v = e^{-2H_y} \text{ and } w = e^{-2H_z} \quad . \tag{27}$$

Using these variables for *u, v* and *w* Eq. (27) reduces to,

$$Z_{(i,j)} = w\left[\frac{\left(u^{|\bar{h}|+1} - v^{|\bar{h}|+1}\right)}{(u-v)} + \frac{\left(\left(u^{|\bar{h}|} + v^{|\bar{h}|}\right)uv\right)}{(1-uv)}\right] \tag{28}$$

Ignoring overhangs and inclusions is appropriate only in the case when $H_z >> H_{x,y}$ (these configurations will lead to additional terms in the partition function which are proportional to e^{-sH_z}, with $s \geq 6$).

The partition function, $Z_{(i,j)}$, exhibits a maximum for $|\bar{h}| = 0$, thus leading to an *upper* bound on H_c ($H_c = J/k_B T_c$) and a *lower* bound on the critical temperature. For this specific case Eq. (28) reduces to

$$Z_{(i,j)} = e^{-2H_z}\left[\frac{1+e^{-2(H_x+H_y)}}{1-e^{-2(H_x+H_y)}}\right] = w\left[\frac{1+uv}{1-uv}\right] \quad . \tag{29}$$

The critical temperature can be found by setting $Z_{(i,j)} = 1$. One finds [28],

$$\sinh(2H_z)\sinh(2(H_x+H_y)) = 1 \quad . \tag{30}$$

By cyclic permutation two similar expressions are found. The difference in these expressions comes from the choice of the wall which has its normal in either the *x, y* or *z* direction. In the anisotropic case it is most convenient to define the domain wall in such a way that the normal of the wall is along the strongest coupling direction. As is evident from Eq. (26) this will lead to a maximum suppression of the contribution of overhangs and inclusions to the partition function. In the asymptotic limit the 3D Ising model gradually converts to the 1D Ising model and the phase transition temperature approaches zero, and thus the expectation value of $\bar{h}$ gradually approaches zero too. However, even for a non-zero value of $\bar{h}$ Eq. (30) is recovered in the asymptotic limit provided that $\bar{h}H_{x,y} << 1$. For sufficiently small values of $H_{x,y}$ all factors $e^{-2\bar{h}H_{x,y}}$ $(=u^{\bar{h}}, v^{\bar{h}})$ in Eq. (28) approach 1 and Eq. (29) will be recaptured.

The critical temperature of the anisotropic 2D Ising ferromagnet is known from Onsager's exact solution [1], i.e. $\sinh(2H_z)\sinh(2H_x)=1$, to vanish asymptotically as

$$2H_z = \left[\ln\left(\frac{H_z}{H_x}\right) - \ln\left(\ln\left(\frac{H_z}{H_x}\right)\right) + O(1) \right] \quad , \tag{31}$$

where the ratio of the exchange energies for bonds parallel to the *x* and z-axes, i.e. $\left(\frac{H_x}{H_z}\right)$, approaches zero [26,27]. Weng, Griffiths and Fisher [26] and Fisher [27] have shown that for the simple cubic lattice an asymptotically exact expression of the same form as Eq. (31) is found with the only modification that H_x is replaced by $H_x + H_y$. The latter provides strong evidence that the

asymptotically exact formula that describes the critical line, between the ferromagnetic and paramagnetic phase in the anisotropic limit, can be written as

$$\sinh(2H_Z)\sinh(2(H_X + H_Y)) = 1$$

.

But this is precisely the result we found in the domain wall analysis. Finally, the value of *O(1)* in Eq. (20) can de determined by comparing Eqs. (20) and (30). We found a value for *O(1)* a value that gradually decreases from ~0.84 at $\left(\frac{H_X + H_Y}{H_Z}\right)$=$10^{-2}$ to ~0.76 at $\left(\frac{H_X + H_Y}{H_Z}\right)$=$10^{-20}$.

Conclusions

We have shown that the boundary tension method leads to the exact criticality conditions of the 2D planar Ising models with nearest neighbour interactions. For the square Ising lattice with nearest and next-nearest neighbour interactions and the anisotropic 3D Ising lattice expressions for the critical temperature are determined.

References

[1]. L. Onsager, *Phys. Rev.* **65**, 117 (1944).

[2]. R.M.F. Houtappel, *Physica* **16**, 435 (1950).

[3]. J. Oitmaa, *J. Phys.* A **14**, 1159 (1981).

[4]. D.P. Landau, *Phys. Rev.* B **21**, 1285 (1980).

[5]. K. Binder and D.P. Landau, *Phys. Rev*. B **21**, 1941 (1980).

[6]. J.M.J. van Leeuwen, *Phys. Rev. Lett*. **34**, 1056 (1975).

[7]. R.H. Swendsen and S. Krinsky, *Phys. Rev. Lett.* **43**, 177 (1979).

[8]. M.P. Nightingale, *Proc. Kon. Ak. Wet.* B **82**, 235 (1979).

[9]. H.W.J. Blöte and M.P. Nightingale, *Physica* A **134**, 274 (1985).

[10]. A. Nihat Berker and K. Hui, *Phys. Rev.* B **48**, 12393 (1993).

[11]. H.W.J. Blöte, A. Compagner and A. Hoogland, *Physica* A **141** (1987) 375.

[12]. E. Müller-Hartmann and J. Zittartz, *Z. Physik* B **27**, 261 (1977).

[13]. T.W. Burkhardt, *Z. Physik* B **31**, 183 (1978).

[14]. B.W. Southern, *Z. Physik* B **30**, 61 (1978).

[15]. H.J.W. Zandvliet, *Europhys. Lett.*, **73** (2006).

[16]. R. Schumann and S. Kobe, *Physics* A 386, 187 (2007).

[17]. M.E. Fisher and A.E. Ferdinand, *Phys. Rev. Lett.* **19** (1967) 169.

[18]. H.J.W. Zandvliet, *Rev. Mod. Phys.* **72**, 593 (2000).

[19]. C. Fan and F.Y. Wu, *Phys. Rev.* **179**, 560 (1969).

[20]. M.P. Nightingale, *Phys. Lett. A* **59**, 486 (1977).

[21]. M.P. Nightingale and H.W.J. Blöte , *J. Phys. A: Math. Gen.* **15**, L33 (1982).

[22]. J. Cardy, *Scaling and Renormalization in Statistical Physics.* Cambridge Univ. Press, Cambridge, (1997).

[23]. A. Pelissetto and E. Vicari, Phys. Rep. **368**, 549 (2002).

[24]. R.B. Griffiths, Phys. Rev. **136**, A437 (1964).

[25]. R. Peierls, Proc. Cambridge Phil. Soc. **32**, 477 (1936).

[26]. C.-Y. Weng, R.B. Griffiths and M.E. Fisher, Phys. Rev. **162**, 475 (1967).

[27]. M.E. Fisher, Phys. Rev. **162**, 480 (1967).

[28]. H.J.W. Zandvliet, A. Saedi and C. Hoede, *Phase Trans. (UK)* **80**, 981 (2007).

Figure captions

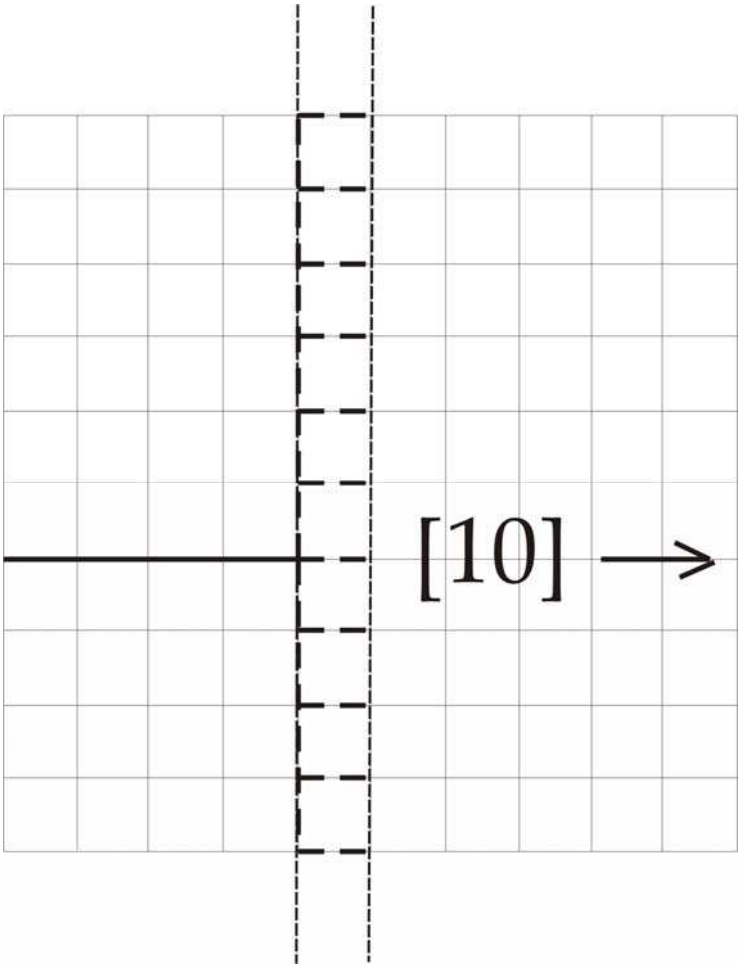

Figure 1

Schematic diagram of a domain wall running along the [10] direction of a square lattice. In the calculation of the boundary tension all possible up and down steps in the domain wall are taken into account. Overhangs and inclusions are omitted in the analysis.

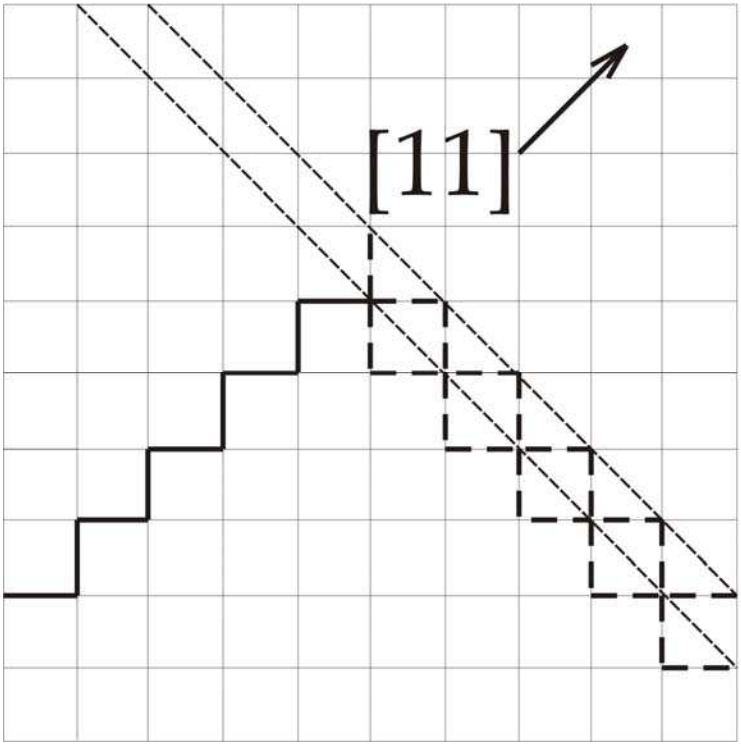

Figure 2

Schematic diagram of a domain wall running along the [11] direction of a square lattice. In the calculation of the boundary tension all possible up and down steps in the domain wall are taken into account. Overhangs and inclusions are omitted in the analysis.

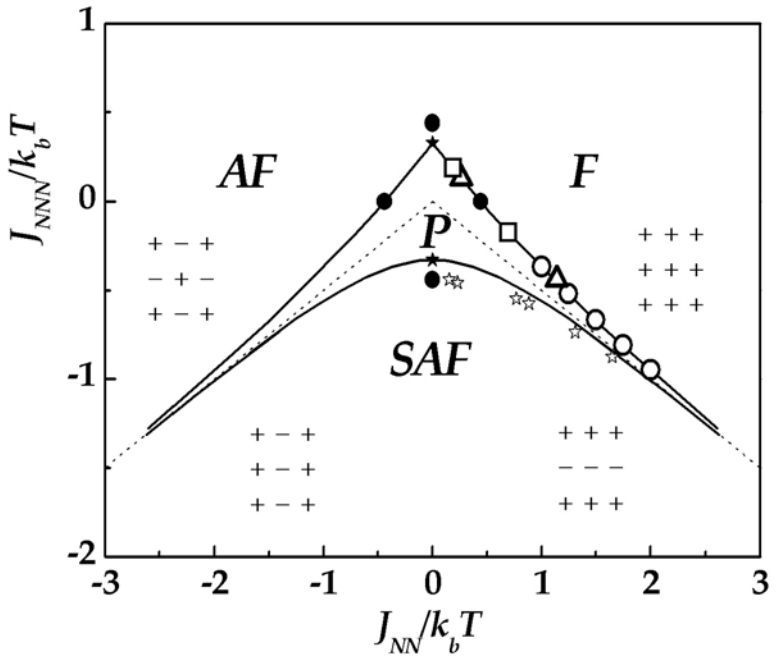

Figure 3

The phase diagram of the isotropic square lattice Ising model with nearest- and next-nearest-neighbor interactions. The solid lines refer to the phase boundaries between the ferromagnetic (*F*), antiferromagnetic (*AF*), superantiferromagnetic (*SAF*) and paramagnetic (*P*) phases as derived in this paper. The data points are series expansions results (triangles, Oitmaa [3]), finite scaling of transfer matrix results (squares, Nightingale [20,21]), Onsager's exact result (filled circle, Onsager [1]), Monte Carlo simulations (open circles, Blöte, Compagner and Hoogland [11] and open stars, Landau [4]) and free-fermion approximation (closed stars, Fan and Wu [19]). The dotted line gives the asymptotic strong-coupling slope ($J_{NNN} \to -\frac{1}{2}|J_{NN}|$).

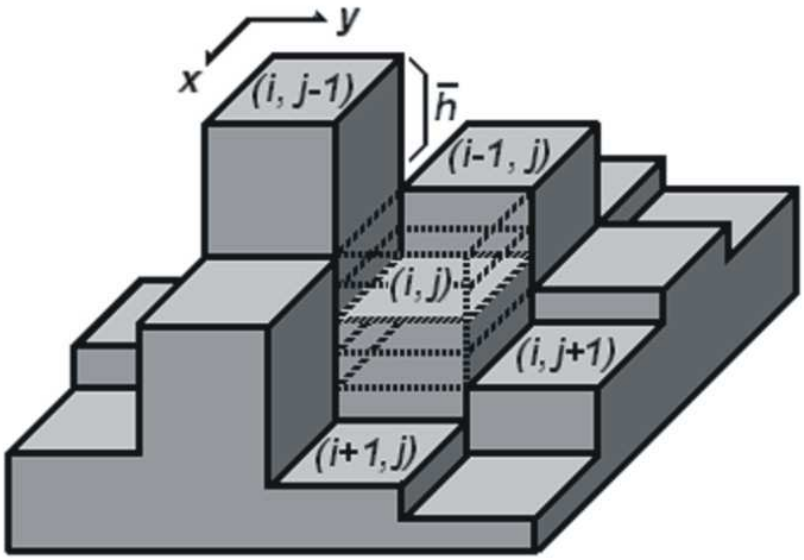

Figure 4

Schematic model of a 2D domain wall of a cubic lattice. The normal of the domain wall is oriented in the *z*-direction. Each column, *h(i,j),* is surrounded by four nearest neighbors labeled *h(i-1,j), h(i,j-1), h(i+1,j)* and *h(i,j+1),* respectively. $\bar{h}$ is the height difference between the *h(i-1,j)* and *h(i,j-1)* columns. $h(i, j) \in [-\infty, \infty]$ ($h(i, j) = 0$ corresponds to the height of the *(i-1,j)-th* column).